PROCEEDINGS OF SCIENCE

Searches for diboson resonances at $\sqrt{s}$ = 13 TeV with the ATLAS detector at the LHC

Daniel Büscher*
University of Freiburg
E-mail: daniel.buescher@cern.ch

Searches for new diboson resonances, carried out with 3.2 fb^{-1} of data taken at $\sqrt{s}$ = 13 TeV with the ATLAS detector at the LHC, are presented. The resonances under consideration are VV ($V = W$ or Z), VH, $\gamma\gamma$ and $Z\gamma$. Most of the searches do not show any significant excess over the expectation from the SM backgrounds. The largest deviation is seen in the invariant diphoton mass spectrum around $m_{\gamma\gamma} = 750$ GeV. It corresponds to a significance of $3.9\,\sigma$ (local) and $2.0\,\sigma$ (global) for a spin-0 resonance with a decay width of $\Gamma/m_{\gamma\gamma} = 6\,\%$.

XXIV International Workshop on Deep-Inelastic Scattering and Related Subjects
11-15 April, 2016
DESY Hamburg, Germany

*On behalf of the ATLAS Collaboration.

PoS(DIS2016)101

1. Introduction

With the increased center-of-mass energy of $\sqrt{s}$ = 13 TeV for Run 2 of the LHC physics beyond the standard model (BSM) might be in reach. New resonances, such as the resonant production of standard model (SM) boson pairs, would be a clear hint of BSM effects. In this article, searches for VV, VH, $\gamma\gamma$ and $Z\gamma$ resonances are discussed, where V can be either a W or Z boson. They are carried out with data taken with the ATLAS detector [1] during the 2015 run of the LHC at $\sqrt{s}$ = 13 TeV, corresponding to an integrated luminosity of 3.2 fb^{-1}.

Simplified models are used as benchmarks for these searches. An extended Higgs sector serves as benchmark model for spin-0 resonances, Heavy Vector Triplets (HVT) [2] for spin-1 (W' and Z') and Randall-Sundrum Gravitons (RSG) [3] for spin-2 resonances.

The searches for W' with masses around $m_{W'} = 2$ TeV are of particular interest. For this signature an excess of 2.5 σ (global) was seen with data taken during the LHC Run 1 at $\sqrt{s}$ = 8 TeV with the ATLAS experiment [4] and 1.8 σ (global) with the CMS experiment [5]. Although these excesses were only seen in particular decay channels, such resonances are not ruled out completely.

Various final states are considered for the searches in Run 2. First, the fully hadronic $VV \to qqqq$ search [6] is presented in Section 2. Further discussed are the semileptonic $VV \to \nu\nu qq$ [7], $VV \to \ell\nu qq$ [8] and $VV \to \ell\ell qq$ [9] searches in Section 3 and the $VH \to \nu\nu bb$, $\ell\nu bb$ and $\ell\ell bb$ searches [10] in Section 4. Finally, searches for $\gamma\gamma$ resonances [11] are presented in Section 5 and $Z\gamma$ resonances [12] in Section 6.

The search strategy is the same for all these analyses. The decay products of a hypothesized resonance are reconstructed and the invariant mass is calculated. The signal is then expected as a peak on top of the continuous SM backgrounds.

2. VV resonances in fully hadronic decay modes

The search for fully hadronic $VV \to qqqq$ resonances employs a so-called *boosted* jet selection. For large invariant diboson masses, m_{VV}, the bosons have large momenta and the two quarks from each $V \to qq$ decay are too close to be reconstructed using two separate jets. Instead, the aim is to reconstruct each V boson in one large-R jet using the anti-k_t algorithm [13] with $R = 1.0$. A *trimming* algorithm [14] is applied to the jets to remove noise from soft radiation.

The event selection requires two large-R jets with $p_{\mathrm{T}} > 450$ (200) GeV for the leading (subleading) jet. A $V \to qq$ tagger [15] is applied, based on the jet mass, m_J, and the jet sub-structure variable D_2 [16, 17]. Further requirements are applied on the number of tracks in the two jets, their rapidity difference and their p_{T} asymmetry. Three overlapping signal regions are defined for WW, WZ and ZZ based on the jet masses.

The SM background, which is mostly QCD multijet production, is described using a power-law function. The background shape is validated using control regions. No significant excess over the background is found in the signal regions, as shown for the WZ selection in Figure 1 (left). The data are interpreted in the HVT and RSG models and 95 % C.L. exclusion limits on the production cross-section $\times$ branching ratio are set, as shown in Figure 1 (right).

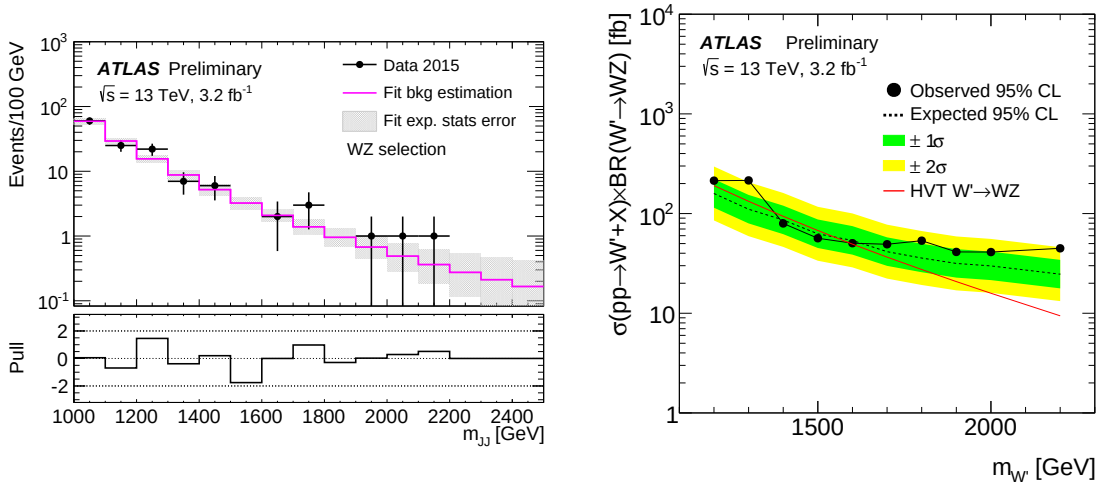

Figure 1: Reconstructed m_{JJ} spectrum for the data and the background model in the fully hadronic VV resonance search with the WZ selection (left). The corresponding limits on the HVT $W' \to WZ$ model are shown on the right (from Reference [6]).

3. VV resonances in semileptonic decay modes

The search for VV resonances in semileptonic decay modes is performed in the zero, one and two-lepton final states, $VV \to \nu\nu qq$, $\ell\nu qq$ and $\ell\ell qq$. The hadronically decaying V boson is reconstructed in a large-R jet with $p_{\mathrm{T}} > 200\,\mathrm{GeV}$ and employing the same boson tagging technique as for the fully hadronic analysis.

The leptonically decaying V boson is reconstructed for the zero-lepton channel by vetoing any leptons in the event and requiring $E_{\mathrm{T}}^{\mathrm{miss}} > 200\,\mathrm{GeV}$. Additional angular cuts on the jets and $E_{\mathrm{T}}^{\mathrm{miss}}$ are applied to reject the multijet background. A veto on b-jets is applied in the zero and one-lepton channels to reject the $t\bar{t}$ background.

The one-lepton channel requires exactly one lepton with tight identification and isolation criteria in the event. Two leptons with looser criteria are required for the two-lepton channel. Both channels require the transverse momenta of the V boson, p_{T}^{V}, and of the jet, p_{T}^{J}, to be larger than $0.4 \cdot m_{VJ}$.

The SM backgrounds are simulated using Monte Carlo (MC) generators and are validated in control regions. No significant excess over the SM backgrounds is observed in the signal regions, as shown for the one-lepton channel with the WZ selection in Figure 2 (left). Limits are set in all three benchmark models. The results for the HVT $W' \to WZ$ model are summarized for all three lepton channels together with the fully hadronic analysis in Figure 2 (right).

4. VH resonances

The search for VH resonance is performed in the leptonic decays of the V boson and the decay of the Higgs boson to b-quarks: $VH \to \nu\nu bb$, $\ell\nu bb$ and $\ell\ell bb$.

The V boson is reconstructed in the zero, one and two-lepton decay channels using similar requirements as for the semileptonic VV search. The Higgs boson is reconstructed using a $H \to bb$

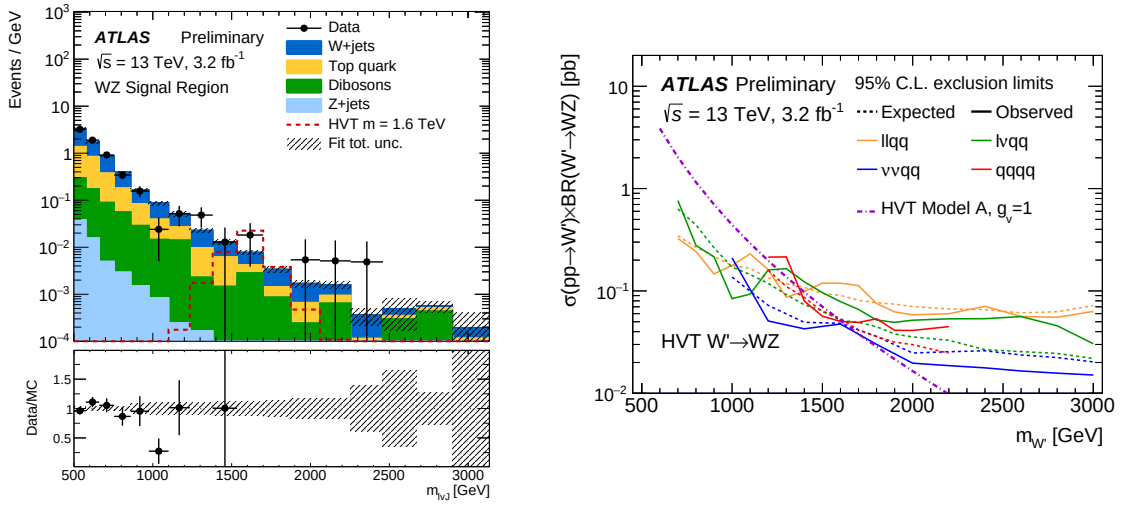

Figure 2: Reconstructed $m_{\ell\nu J}$ spectrum for the data and the backgrounds in the semileptonic VV resonance search for the one-lepton channel [8] with WZ selection (left). The corresponding limits on the HVT $W' \to WZ$ model are shown on the right together with the other semileptonic channels and the ones from the fully hadronic search [18].

tagger [19]. It uses the b-tagging algorithm MV2c20 [20, 21] applied to track jets with $R = 0.2$, which are ghost-associated to a large-R jet, to define one and two-tag regions. The signal region is defined by applying a cut on the jet mass of $75 < m_J < 145\,\text{GeV}$. The mass side-bands and additional b-tags in the event are used to define control regions.

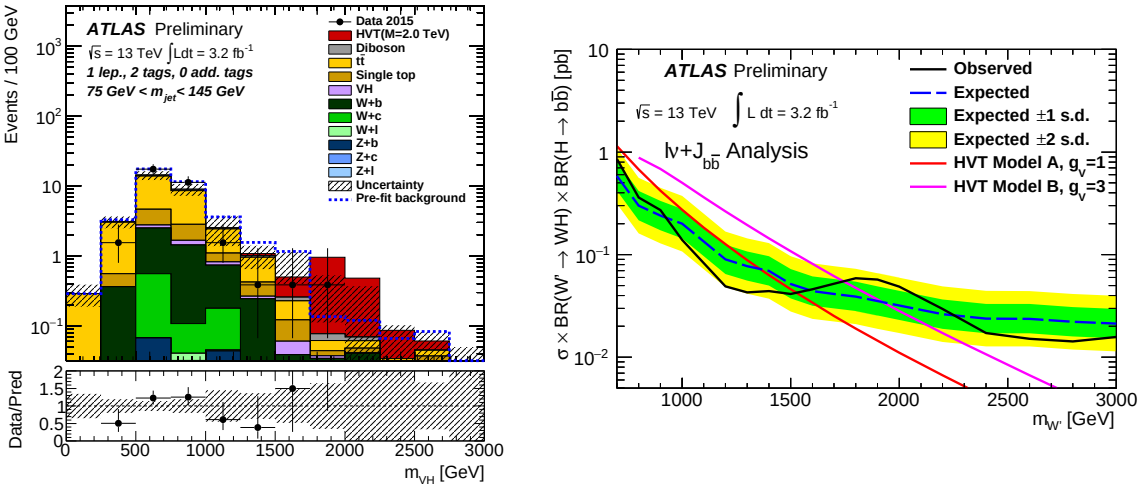

Figure 3: Reconstructed m_{VH} spectrum for the data and the backgrounds in the VH resonance search with one-lepton, two-tag selection (left). The corresponding limits on the HVT $W' \to WH$ model are shown on the right (from Reference [10]).

The SM backgrounds are simulated with MC and are validated in control regions. No significant excess over the SM background is observed in the signal regions, as shown for the one-lepton channel and two-tag region in Figure 3 (left). Limits are set in the HVT model and are shown for the one-lepton channel in Figure 3 (right).

5. $\gamma\gamma$ resonances

The search for diphoton resonances is carried out under spin-0 and spin-2 hypotheses. Two photons with tight identification and isolation criteria are selected. They are required to be within the precision region of the calorimeter of $|\eta| < 2.37$, excluding $1.37 < |\eta| < 1.52$.

The spin-0 analysis is optimized for a Higgs-boson like signal. The photons are required to fulfill $E_{\mathrm{T}}^{\gamma 1} > 0.4 \cdot m_{\gamma\gamma}$ and $E_{\mathrm{T}}^{\gamma 2} > 0.3 \cdot m_{\gamma\gamma}$. Limits are given on the fiducial cross section in the search range of $200\,\mathrm{GeV} \leq m_X < 2\,\mathrm{TeV}$ and $0\,\% < \Gamma_X/m_X \leq 10\%$, where Γ_X is the decay width of the hypothesized resonance X.

The spin-2 analysis employs a looser selection by requiring $E_{\mathrm{T}}^{\gamma 1,2} > 55\,\mathrm{GeV}$. The data is interpreted in the RSG model in a search range of $500\,\mathrm{GeV} \leq m_X < 3\,\mathrm{TeV}$ and $0.01 \leq \kappa/\overline{M}_{Pl} \leq 0.3$, which corresponds to approximately $0\,\% < \Gamma_X/m_X \leq 10\%$.

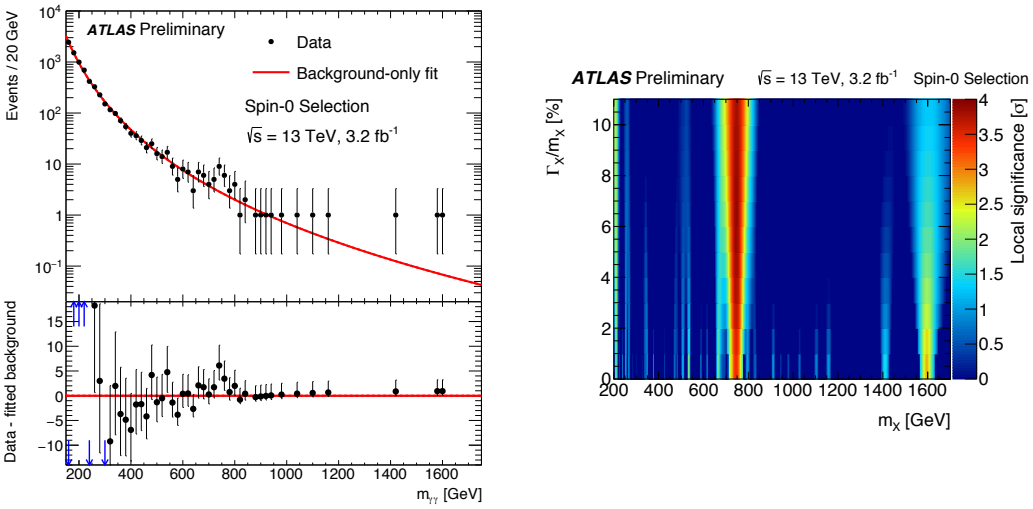

Figure 4: Reconstructed $m_{\gamma\gamma}$ spectrum for the data and the background model in the $\gamma\gamma$ resonance search with spin-0 selection (left). The corresponding local significance as function of the resonance mass and width are shown on the right (from Reference [11]).

The background for the spin-0 analysis is modeled using a family of nested functions (power law times logarithmic polynomials) and the required degrees of freedom are determined from an F-test. The background is compared to the data in the signal region in Figure 4 (left). An excess over the background can be seen around $m_{\gamma\gamma} = 750\,\mathrm{GeV}$. The excess corresponds to a maximum local significance of $3.9\,\sigma$ assuming $m_X = 750\,\mathrm{GeV}$ and $\Gamma_X/m_X = 6\,\%$, as shown in Figure 4 (right). For a narrow resonance with the same mass the local significance is slightly lower with $3.5\,\sigma$. Taking the look-elsewhere effect into account, the excess corresponds to a global significance of $2.0\,\sigma$ for $\Gamma_X/m_X = 6\,\%$ in the search range.

A similar procedure is applied in the spin-2 analysis, resulting in slightly lower significances of $3.6\,\sigma$ (local) and $1.8\,\sigma$ (global) for $m_X = 750\,\mathrm{GeV}$ and $\kappa/\overline{M}_{Pl} = 0.2$ ($\Gamma_X/m_X \simeq 6\,\%$).

The compatibility of the excess with the Run 1 data is estimated [11]. For the spin-0 assumption a $1.9\,\sigma$ local excess is observed in the $\sqrt{s} = 8\,\mathrm{TeV}$ data at $m_X = 750\,\mathrm{GeV}$, assuming $\Gamma_X/m_X = 6\,\%$. This corresponds to a compatibility of $1.2\,\sigma$ with the $\sqrt{s} = 13\,\mathrm{TeV}$ data for the production of the resonance in the gluon-fusion mode. Here, the cross section scales with a factor

4.7 due to the increased center of mass energy. For quark-induced production the scaling is only 2.7, resulting in a lower compatibility of 2.1 σ.

No significant excess is observed in the $\sqrt{s} = 8\,\text{TeV}$ data for the spin-2 hypothesis, resulting in lower compatibilities of 2.7 σ for the gluon-fusion mode and 3.3 σ for the quark-induced production.

6. $Z\gamma$ resonances

Searches for $Z\gamma$ are particularly interesting in the presence of a possible $\gamma\gamma$ resonance signal. They are carried out in the leptonic $Z \to \ell\ell$ decay mode for masses of $0.25 \leq m_X \leq 1.5\,\text{TeV}$ and in the hadronic $Z \to qq$ for masses of $0.72 \leq m_X \leq 2.75\,\text{TeV}$.

The leptonic channel requires a photon with $E_T^\gamma > 0.3 m_X$ and two leptons with $p_T^\ell > 10\,\text{GeV}$ and $m_{\ell\ell} - m_Z < 15\,\text{GeV}$. The hadronic channel requires $E_T^\gamma > 250\,\text{GeV}$ and a large-R jet with $p_T^J > 200\,\text{GeV}$ and $80 < m_J < 110\,\text{GeV}$.

An analytic model is employed for the SM backgrounds, similar to the $\gamma\gamma$ spin-0 analysis. Limits are set on a heavy Higgs-boson model. No excess over the backgrounds is observed.

7. Summary

Several searches for diboson resonances have been carried out with data taken in 2015 at $\sqrt{s} = 13\,\text{TeV}$ with the ATLAS experiment at the LHC. From the analyses discussed here, only the $\gamma\gamma$ resonance search sees an excess over the SM backgrounds. It corresponds to a significance of 3.9 σ (local) and 2.0 σ (global) for a broad spin-0 resonance with a decay width of $\Gamma/m_{\gamma\gamma} = 6\,\%$. For a narrow resonance or the spin-2 hypothesis the significances are slightly lower. The other diboson searches see good agreement of the data with the standard model prediction.

References

[1] ATLAS Collaboration, *The ATLAS Experiment at the CERN Large Hadron Collider*, JINST **3** (2008) S08003.

[2] D. Pappadopulo, A. Thamm, R. Torre, and A. Wulzer, *Heavy vector triplets: bridging theory and data*, Journal of High Energy Physics **9** (2014) 60, arXiv:1402.4431 [hep-ph].

[3] K. Agashe, H. Davoudiasl, G. Perez, and A. Soni, *Warped gravitons at the CERN LHC and beyond*, Phys. Rev. **D76** (2007) 036006, hep-ph/0701186.

[4] ATLAS Collaboration, *Combination of searches for WW, WZ, and ZZ resonances in pp collisions at $\sqrt{s}$ = 8 TeV with the ATLAS detector*, Physics Letters B **755** (2016) 285–305, arXiv:1512.05099.

[5] CMS Collaboration, *Search for massive WH resonances decaying into the l nu b anti-b final state at $\sqrt{(s)} = 8$ TeV*, arXiv:1601.06431.

[6] ATLAS Collaboration, *Search for resonances with boson-tagged jets in 3.2 fb^{-1} of pp collisions at $\sqrt{s}$ = 13 TeV collected with the ATLAS detector*, ATLAS-CONF-2015-073. https://cds.cern.ch/record/2114845.

[7] ATLAS Collaboration, *Search for diboson resonances in the $\nu\nu qq$ final state in pp collisions at $\sqrt{s}$ =13 TeV with the ATLAS detector*, ATLAS-CONF-2015-068. https://cds.cern.ch/record/2114840.

[8] ATLAS Collaboration, *Search for WW/WZ resonance production in the $\ell\nu qq$ final state at $\sqrt{s} = 13$ TeV with the ATLAS detector at the LHC*, ATLAS-CONF-2015-075. https://cds.cern.ch/record/2114847.

[9] ATLAS Collaboration, *Search for diboson resonances in the llqq final state in pp collisions at $\sqrt{s}$ = 13 TeV with the ATLAS detector*, ATLAS-CONF-2015-071. https://cds.cern.ch/record/2114843.

[10] ATLAS Collaboration, *Search for new resonances decaying to a W or Z boson and a Higgs boson in the $\ell\ell b\bar{b}$, $\ell\nu b\bar{b}$, and $\nu\nu b\bar{b}$ channels in pp collisions at $\sqrt{s} = 13$ TeV with the ATLAS detector*, ATLAS-CONF-2015-074. https://cds.cern.ch/record/2114846.

[11] ATLAS Collaboration, *Search for resonances in diphoton events with the ATLAS detector at $\sqrt{s}$ = 13 TeV*, ATLAS-CONF-2016-018. https://cds.cern.ch/record/2141568.

[12] ATLAS Collaboration, *Search for heavy resonances decaying to a Z boson and a photon in pp collisions at $\sqrt{s} = 13$ TeV with the ATLAS detector*, ATLAS-CONF-2016-010. https://cds.cern.ch/record/2139795.

[13] M. Cacciari, G. P. Salam, and G. Soyez, *The anti-k_t jet clustering algorithm*, Journal of High Energy Physics **4** (2008) 063, arXiv:0802.1189.

[14] D. Krohn, J. Thaler, and L.-T. Wang, *Jet trimming*, Journal of High Energy Physics **2** (2010) 84, arXiv:0912.1342.

[15] ATLAS Collaboration, *Identification of boosted, hadronically-decaying W and Z bosons in $\sqrt{s} = 13$ TeV Monte Carlo Simulations for ATLAS*, ATL-PHYS-PUB-2015-033. https://cds.cern.ch/record/2041461.

[16] A. J. Larkoski, I. Moult, and D. Neill, *Power counting to better jet observables*, Journal of High Energy Physics **12** (2014) 9, arXiv:1409.6298.

[17] A. J. Larkoski, I. Moult, and D. Neill, *Analytic Boosted Boson Discrimination*, arXiv:1507.03018.

[18] ATLAS Collaboration, *Summary plots from the ATLAS Exotic physics group*, https://atlas.web.cern.ch/Atlas/GROUPS/PHYSICS/CombinedSummaryPlots/EXOTICS/.

[19] ATLAS Collaboration, *Expected Performance of Boosted Higgs ($\rightarrow b\bar{b}$) Boson Identification with the ATLAS Detector at $\sqrt{s} = 13$ TeV*, ATL-PHYS-PUB-2015-035. https://cds.cern.ch/record/2042155.

[20] ATLAS Collaboration, *Performance of b-jet identification in the ATLAS experiment*, Journal of Instrumentation **11** (2016) P04008, arXiv:1512.01094.

[21] ATLAS Collaboration, *Expected performance of the ATLAS b-tagging algorithms in Run-2*, ATL-PHYS-PUB-2015-022. http://cds.cern.ch/record/2037697.